Protein Engineering vol. 16 no. 5 pp. 351–356, 2003
DOI: 10.1093/protein/gzg048

The structural basis of Trp192 and the C-terminal region in trichosanthin for activity and conformational stability

Yi Ding[1,2], Hiumei Too[3], Zhilong Wang[1], Yiwei Liu[1], Mark Bartlam[1], Yicheng Dong[1,2], Kambo Wong[3], Pangchui Shaw[3,4] and Zihe Rao[1,2,4]

[1]Laboratory of Structural Biology and the MOE Laboratory of Protein Science, School of Life Science and Engineering, Tsinghua University, Beijing 100084, [2]Institute of Biophysics, Chinese Academy of Science, Beijing 100101 and [3]Department of Biochemistry, Chinese University of Hong Kong, Hong Kong, China

[4]To whom correspondence should be addressed.
E-mail: pcshaw@cuhk.edu.hk; raozh@xtal.tsinghua.edu.cn

Y.Ding and H.Too contributed equally to this work

Trichosanthin (TCS) is a type I ribosome-inactivating protein (RIP) possessing *N*-glycosidase activity. TCS has various pharmacological properties, including immunomodulatory, anti-tumor and anti-HIV activities. Up to seven C-terminal residues of TCS (TCS-C7) can be deleted resulting in lower antigenicity with minimal effects on its activity. However, an additional problem is that the minimal effects on activity are higher than the reduction in antigenicity. In the present work, the crystal structure of TCS-C7 was determined. It shows the details of the C-terminal residues of TCS-C7, and in particular the hydrogen bonds between P35 and L240, S196 and L240, and W192 and L239, which play an important role in maintaining the structure of TCS-C7. Further analysis shows that the hydrogen bonds related to Leu240 are key in maintaining the relationship between N- and C-terminal domains. The major role of the C-terminal tail appears to stabilize the structure of TCS. The conformation between helix H7 at the N-terminal domain and the C-terminal tail at the C-terminal domain is also revealed. Two mutants, TCS-W192F and TCS-C7-W192F, were prepared and crystal structures were determined. These variants have greatly reduced ribosome-inactivating activities compared with TCS and TCS-C7, respectively, and TCS-W192F and TCS-C7-W192F have a similar stability in guanidine hydrochloride compared with TCS-C7. This suggests that Trp192 can affect the ribosome-inactivating activity of TCS.

Keywords: conformational stability/ribosome-inactivating proteins/trichosanthin/W192F

Introduction

Ribosome-inactivating proteins (RIPs) are a group of cytotoxins, which possess a unique rRNA *N*-glycosidic activity by hydrolyzing a single *N*-glycoside bond between adenine and ribose at A4324 in the 28S rRNA of rat liver ribosomes. This damages the ribosomes irreversibly with the consequent arrest of protein synthesis (Endo and Tsurugi, 1987; Endo *et al*., 1987; Stirpe *et al*., 1988). They are abundant and widely distributed in higher plant species. RIPs can be classified into type I and type II. Type I RIPs are basic, single-chain proteins with molecular weights of ~30 kDa. They are potent inhibitors of protein synthesis in the cell-free system. Unlike type II RIPs, type I RIPs are single-chain proteins without B chain. As a result, they are relatively non-toxic to the intactness of the whole cell. Type II RIPs consist of a catalytically active A chain linked to a carbohydrate-binding B chain by a disulfide linkage. The A chain is homologous with type I RIP and is responsible for the toxicity of the molecule. The B chain possesses lectin properties which facilitate entry of the A chain into the cytoplasm of the cell (Li *et al*., 1999).

Trichosanthin (TCS) is a type I RIP isolated from the root tuber of *Trichosanthes kirilowii* Maximowicz (Jimenez and Vazquez, 1985; Stirpe and Barbieri, 1986; Zhang and Wang, 1986; Yeung *et al*., 1988). It has 247 amino acids and can inactivate eukaryotic ribosomes via its *N*-glycosidase activity. It possesses a large N-terminal domain, residues 1–202 and a small C-terminal domain, residues 203–247 (Stirpe and Barbieri, 1986). The active pocket responsible for *N*-glycosidase activity is located in the cleft between the two domains (Gao *et al*., 1994). TCS has been used extensively for inducing mid-term abortion and treating ectopic pregnancies, hydatidiform and trophoblastic moles in China (Huang, 1987; Lu and Jin, 1990). In recent years, TCS had also been found to possess various pharmacological properties including immunomodulatory, anti-tumor and anti-HIV activities (Shaw *et al*., 1994). Clinical trials have been performed, with resulting increases of $CD4^+$ and $CD8^+$ T cells in patients (McGrath *et al*., 1989; Byers *et al*., 1990).

Although TCS is effective in killing tumor cells *in vivo* and *in vitro*, its side effects on patients have not been systematically evaluated. In the long run, it would be useful if the antigenicity of TCS could be reduced and its half-time *in vivo* increased. It is possible to reduce the antigenicity of TCS by site-specific coupling of PEG modification (PEGylation) (He *et al*., 1999) or by deleting the C-terminal residues (Chan *et al*., 2000). Reducing molecular weight could also reduce its antigenicity (Chan *et al*., 2000). TCS-C7, generated by deleting the last seven C-terminal amino acid residues, has a 2.7-fold decrease in antigenicity compared with TCS. Although the *in vitro* ribosome-inactivation activity and *in vivo* cytotoxicity towards K562 cells have decreased by 10-fold from the wild type (WT), it is still a potent RIP that is effective in the nanomolar range (Chan *et al*., 2000). On the other hand, it is interesting to note that mutants with more than seven residues deleted from the C-terminus are expressed as inclusion body, and fail to refold under the influence of urea or guanidine hydrochloride (GnHCl) (Chan *et al*., 2000).

In order to explore the role of the C-terminal residues, the crystal structure of TCS-C7 has been determined and compared with the structure of the wild-type TCS (WT-TCS). Further protein engineering based on the structure was performed, with the result that the mutation of Trp192 greatly decreased the

ribosome-inactivating activity and stability of TCS. The crystal structures of TCS-W192F and TCS-C7-W192F were also determined.

Materials and methods

Construction of TCS-C7 expression vectors and protein purification

The expression vectors were constructed by Chan *et al*. (Chan *et al*., 2000). Protein expression and purification were performed as described previously (Wong *et al*., 1994).

Mutation and expression of TCS-W192F and TCS-C7-W192F

A site-directed mutant at position 192 of TCS and the deletion mutant TCS-C7 were generated by PCR mutagenesis using *Pfu* DNA polymerase (Strategene) on pET8C carrying the WT-TCS and TCS-C7 sequences, respectively. The PCR product was cleaved by *Nco*I and *Bam*HI and cloned to pET8C for expression. The mutations were confirmed by DNA sequencing. Single colony was innoculated to 2 l of M9ZB medium containing 50 μg/ml ampicillin and 25 μg/ml chloramphenicol at 37°C until OD_{600} reached 0.6–0.8 and the protein was induced by 0.4 mM IPTG at 25°C for 3–4 h. The protein was purified with an 8 × 2.5 cm CM-Sepharose CL6B column (Amersham Pharmacia Biotech) followed by a HiTrap SP-Sepharose fast flow column (Amersham Bioscience) using 20 mM phosphate buffer with a 0–1 M NaCl gradient.

Crystallization

Crystals of TCS-C7 were grown by the hanging-drop vapor diffusion method with a protein concentration of ~20 mg/ml. The reservoir contained 100 mM CaCodylate, pH 6.5, 200 mM $CaOAc_2$ and 15% PEG8000 (Li *et al*., 2002). The crystallization condition of TCS-C7-W192F was similar to TCS-C7. Crystals of TCS-W192F were grown according to the crystallization condition of WT-TCS (Gao *et al*., 1994). The protein concentration was ~40 mg/ml, and the reservoir contained 100 mM NaOAc–HOAc, pH 4.5, 100 mM $CaCl_2$ and 20% KCl.

Diffraction and data collection

Diffraction data of the crystals were collected at 100 K on an in-house Mar345 image plate with a Rigaku rotating Cu Kα anode X-ray generator at 48 kV and 98 mA (λ = 1.5418 Å). The crystals of TCS-C7 and TCS-C7-W192F belong to space group $P2_1$ with four protein molecules in the asymmetric unit, while the crystals of TCS-W192F belong to space group $P2_12_12_1$ with one protein molecule in the asymmetric unit. Indexing and integration of all images were performed in DENZO and scaling of the intensity data was performed in SCALEPACK; both are from the HKL program package (Otwinowski and Minor, 1997). The crystal parameters and data collection statistics are listed in Table I.

Structure determination and refinement

TCS-C7. Molecular replacement. The TCS-C7 structure was solved by the molecular replacement method. The processing was carried out with CNS (Brunger *et al*., 1998) using the TCS-NADPH complex (PDB code 1TCS) molecule as a search model. The NADPH molecule and all water molecules were discarded and the temperature factors of all remaining atoms were fixed at 20.0 $Å^2$. The rotation and translation function calculation was carried out using the data in the resolution range 15–3.5 Å. According to the self-rotation function, it

Table I. Data collection and refinement statistics

	TCS-C7	TCS-W192F	TCS-C7-W192F
Resolution (Å)	50–2.0	50–2.0	50–2.0
Space group	$P2_1$	$P2_12_12_1$	$P2_1$
Unit cell parameters			
a (Å)	71.6	37.8	72.0
b (Å)	74.4	74.7	74.5
c (Å)	87.6	78.4	88.0
β (°)	96.9		97.1
Total number of reflections	22 6719	73 184	409 193
Number of unique reflections	70 850 (6753)	15 441 (1473)	57 330 (5958)
$I / \sigma (I)$	10.4 (5.1)	12.6 (6.6)	14.0 (7.4)
Redundancy	3.2 (3.1)	4.7 (4.5)	7.1 (6.4)
R_{merge}[a] (%)	7.1 (24.8)	8.5 (28.8)	8.5 (35.1)
Completeness (%)	98.2 (95.8)	99.0 (97.5)	96.2 (91.8)
R-factor	0.174	0.186	0.223
R_{free}[b]	0.234	0.248	0.283
R.m.s. bond length deviation (Å)	0.014	0.017	0.018
R.m.s. bond angle deviation (°)	1.62	1.76	1.84
Solvent molecules	1120	160	636
Average *B*-factor ($Å^2$)			
Total	16.6	12.5	14.1
Main-chain atoms	18.9	15.4	17.9
Side-chain atoms			
Ramachandran plot for non-glycine and non-proline residues[c]			
Most favored regions (%)	91.0	92.5	89.9
Additional allowed regions (%)	8.2	7.5	9.7
Generously allowed regions (%)	0.8	0	0.5
Disallowed regions (%)	0	0	0

Numbers in parentheses correspond to the highest resolution shell (2.07–2.0 Å).
[a]$R_{merge} = \Sigma_{hkl} |I_i - I_m| / \Sigma_{hkl} I_{m,}$ where I_i and I_m are the observed intensity and the mean intensity of related reflections, respectively.
[b]Ten percent of the total reflections were used for R_{free} calculation.
[c]The quality of the structures of one molecule in the asymmetric unit was assessed using PROCHECK and statistics are given for the monomer.

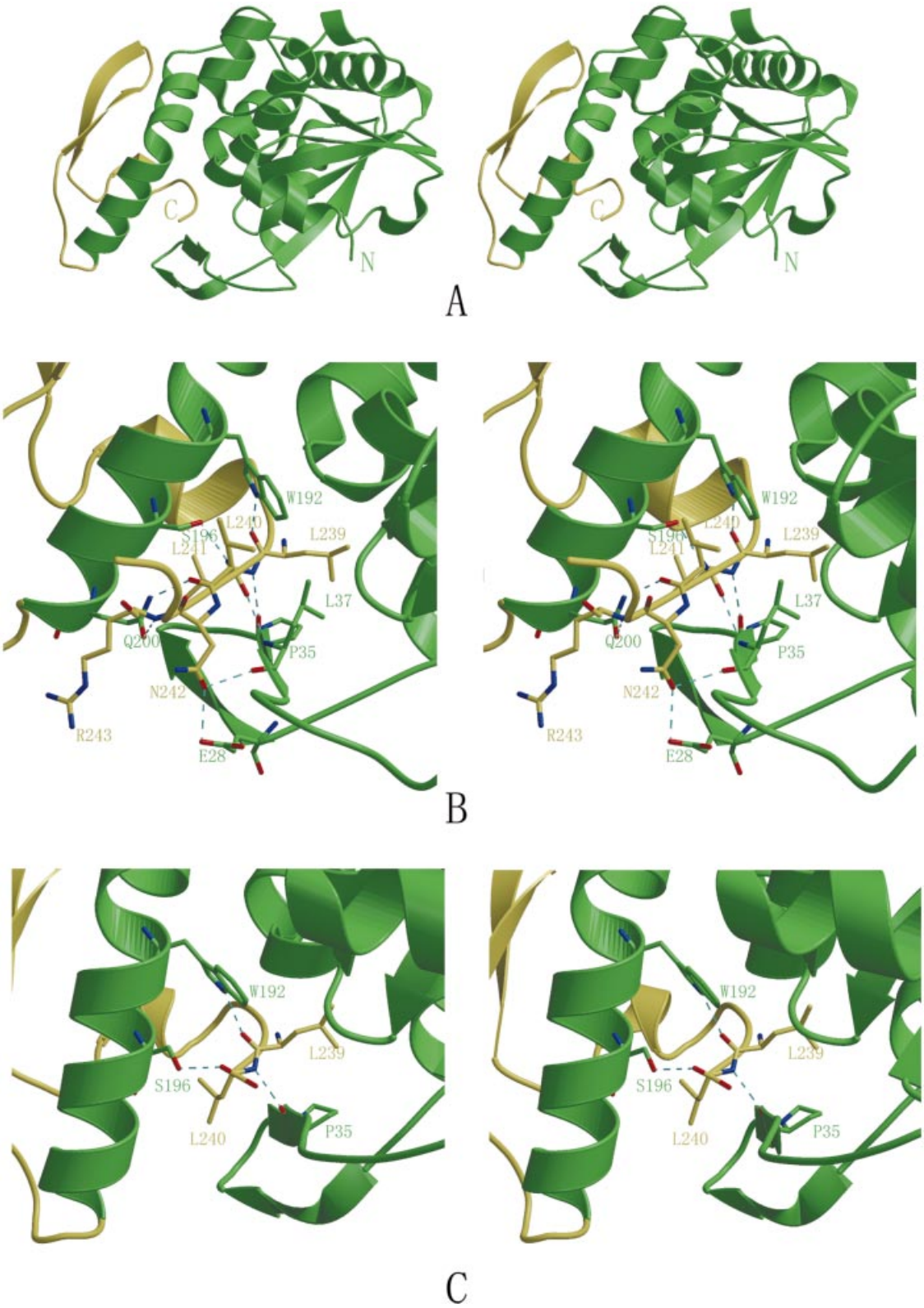

Fig. 1. Structural presentation of the hydrogen bonds in TCS and TCS-C7. (**A**) Stereoview of the TCS-C7 structure. Two domains: N-domain (large domain, green) and C-domain (small domain, yellow). (**B**) Stereoview of the hydrogen bonds formed by the C-terminal residues of TCS. (**C**) Stereoview of the hydrogen bonds formed by the C-terminal residues of TCS-C7.

appeared there were four molecules in an asymmetric unit. Finally, four molecules were located in an asymmetric unit just as predicted and the molecular packing in the unit cell is plausible.

Crystallographic refinement. The model was rebuilt with O (Jones *et al*., 1991) and refined with CNS. No data truncation was applied in the refinement. Ten percent of the data were set aside in order to calculate the free *R*-factor. After a rigid body

refinement, the *R*-value dropped to 0.373 and R_{free} was 0.403 for the data in the resolution range 40–3 Å. The last seven residues were deleted from the protein structure and this model was then refined by simulated annealing using data in the resolution range 40–2.5 Å. A starting temperature of 5000 K was gradually decreased to 300 K in steps of 50 K. At this stage, the *R*-factor and R_{free} were 0.262 and 0.317, respectively. Using the 40–2.0 Å data, $2|F_o| - |F_c|$ and $|F_o| - |F_c|$ electron density maps were calculated and examined in O. The refinement was completed by alternating between manual building and minimization using data in the resolution range 40–2.0 Å. Group B-factor refinement was then used to refine the temperature factors in the model. In each refinement step, initial anisotropic overall B-factor correction with a lower resolution limit of 6 Å and bulk-solvent correction were applied to the data. 1120 water molecules were located automatically with CNS. The water molecules with thermal factors higher than 50 $Å^2$ were removed.

TCS-W192F and TCS-C7-W192F. Since the crystal of TCS-W192F is isomorphous with WT-TCS and the crystal of TCS-C7-W192F is isomorphous with TCS-C7, the $2|F_o| - |F_c|$ and $|F_o| - |F_c|$ difference electron density maps were calculated by the difference Fourier method with the collected diffraction data as F_o and the structure of the isomorphous model as F_c. Most of the residues fit well in the $2|F_o| - |F_c|$ map. When W192 was omitted from the $2|F_o| - |F_c|$ and $|F_o| - |F_c|$ maps, the side chain is like a phenyl ring. This suggested that W192 has been mutated to Phe. As a result, W192 was changed to Phe for further refinement using the program O. Refinement of the two structures was also performed using CNS. In each case, the refinement was completed by alternating between manual building and minimization using data in the resolution range 40–2.0 Å.

Ribosome-inactivating activity assay

The ribosome-inactivating activity assay was determined by an *in vitro* translation system using rabbit reticulocyte lysate (Promega), as previously described (Chan *et al*., 2000).

GnHCl denaturation

CD spectra in the peptide region (190–260 nm) were measured with a Jasco J-810 spectropolarimeter at 37°C. Protein samples (10 mM) were treated with GnHCl concentrations between 0.0 and 7.0 M in 20 mM phosphate buffer, pH 6.7. The protein samples were equilibrated with GnHCl solution for 30 min. Each protein was scanned three times from 190 to 260 nm and the spectra were averaged, subtracted from buffer blank spectrum and expressed as residual molar ellipticity (RME) with adjustment of the number of amino acid residues of each variant proteins. The RME at 222 nm, the prominent band contributed by the secondary structure, was plotted against different concentrations of GnHCl.

Results

Quality of the crystal structures

The refinement statistics are listed in Table I. The atomic positions of every residue were verified by the omit electron density map. After refinement, the *R*-factor and r.m.s.d. of bond length and bond angle of these structures are rational. The program PROCHECK (Laskowski *et al*., 1993) was used to check the stereochemistry of the structures: the Ramachandran plot shows that 91.0, 92.5 and 89.9% of the non-glycine and non-proline residues fall in the core region in TCS-C7, TCS-W192F, TCS-C7-W192F structures, respectively; the remainder are in the allowed region and no residues were found in the disallowed region.

Table II. Hydrogen bonds bridging N- and C-terminal domains in TCS and TCS-C7

	Hydrogen bond		Distance (Å)
	N-terminal atom	C-terminal atom	
WT-TCS (i)	Leu-37 O	Asn242 OD1	3.15
	Glu28 OE1	Asn242 OD1	2.98
	Leu37 N	Leu240 O	2.95
	Pro35 O	Leu240 N	2.97
WT-TCS (ii)	Gln200 OE1	Arg243 N	3.00
	Gln200 NE2	Leu241 O	2.76
	Ser196 OG	Leu241 N	2.87
	Trp192 NE1	Leu239 O	2.87
TCS-C7	Pro35 O	Leu240 N	2.86
	Trp192 NE1	Leu239 O	2.95
	Ser196 OG	Leu240 O or Leu240 OH	2.68

Hydrogen bonds bridging N- and C-terminal domains are lost in TCS-C7

The overall structure of TCS-C7 is displayed as a ribbon diagram in Figure 1A. The Cα r.m.s.d.s between TCS-C7 and WT-TCS are small, suggesting there are no significant structural differences between TCS-C7 and WT-TCS, except that TCS-C7 has a shortened C-terminus.

The C-terminal tail of TCS, sandwiched between helix 7 and the β-hairpin formed by strands 2 and 3, serves to connect the N-terminal domains (1–202) and the C-terminal domains (203–247) of TCS together. A number of hydrogen bonds link the C-terminal tail to the N-terminal domain. They can be classified into two groups: (i) hydrogen bonds that link to the β-hairpin; and (ii) hydrogen bonds that link to helix 7 (Table II) (Figure 1B). While in TCS-C7, all of these hydrogen bonds, except for those between Leu239 O … Trp192 NE1 and Leu240 N … Pro35 O, were removed by deleting the last seven residues. In TCS-C7, one of the C-terminal oxygen atoms occupies the void left by Leu241 N and forms a hydrogen bond to Ser196 OG, replacing the hydrogen bond Ser196 OG … Leu241 N in WT-TCS (Figure 1C).

The solvent accessible surface areas of Trp192 calculated for TCS-C7 and WT-TCS are 23.08 and 11.26 $Å^2$, respectively. This result agrees with our previous observation that the fluorescence spectrum of C7 was red-shifted, suggesting a high solvent exposure for the fluorophore Trp192.

Structures of the W192F mutants

Trp192 is an invariant residue within the RIP family. To observe the effect of removing the hydrogen bond in Trp192, it was replaced by Phe in WT-TCS and TCS-C7. In the structures of TCS-W192F and TCS-C7-W192F, Phe192 fits their electron density maps well. In order to reveal the effects of the W192F mutation, the TCS, TCS-C7, TCS-W192F and TCS-C7-W192F structures were superimposed. The r.m.s.d.s among them were all in the range 0.2–0.6 Å. No major structural changes were observed upon mutation of W192F.

Ribosome-inactivating activities of TCS mutants

The ribosome-inactivating activities of TCS mutants were WT-TCS (IC_{50} = 0.17 nM), TCS-C7 (IC_{50} = 1.8 nM), TCS-W192F (IC_{50} = 1.3 nM), TCS-C7-W192F (IC_{50} = 10 nM). The activities of both TCS-C7 and TCS-W192F decreased ~10- and

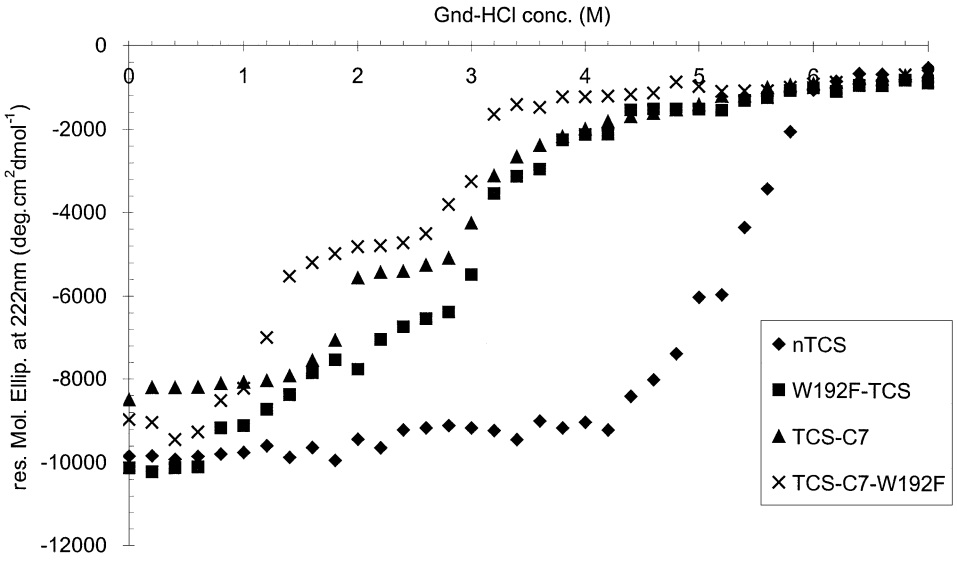

Fig. 2. GnHCl unfolding curve. Proteins were equilibrated with different concentrations of GnHCl for 30 min before the measurement of CD spectra at 37°C from 190 to 260 nm.

~7-fold, respectively. The effect of deletion of the C-terminal residues and W192F appeared to be cumulative—the TCS-C7-W192F mutant has a ~60-fold reduction in activity.

Destabilized C7 mutants unfold via an intermediate state

The unfolding of WT-TCS follows an apparent two-state model, in which only the folded or the completely unfolded states exist. However, for TCS-C7, a plateau of the unfolding curve was observed at ~2–3 M GnHCl, indicating the presence of a partially structured intermediate (Figure 2). Judging by the RME at 222 nm, the intermediate state retained ~75% helical content. Intermediate states were also observed for TCS-C7-W192F and, to a lesser extent, TCS-W192F. Although quantification of thermodynamic parameters is not possible for non-two-state systems, the relative stability of TCS and mutants was found to be WT > W192F > C7 > C7-W192F. Both the deletion of the C-terminal residues and the mutation of W192F destabilized TCS.

Discussion

Role of Trp192

Mutagenesis of Trp192 to Phe has resulted in variants with a significant reduction in conformational stability and a decrease in ribosome-inactivating activity. The NE1 of Trp192 forms a hydrogen bond with the main chain O atom of the residue Leu239. Moreover, the indole ring of Trp192 forms hydrophobic interactions with the side chains of Arg163 and Leu241. The large reduction in stability is likely due to the removal of these interactions as a result of the W192F mutation.

Trp192 is one of the few residues around the active pocket that are invariant throughout the RIP family, including the ricin A chain (Katzin *et al*., 1991). Mutation of the corresponding Trp to Phe in ricin A also results in a less active variant (Bradley and McGuire, 1990). Trp192 in TCS forms the bottom of the hydrophobic cavity and is involved in the definition of the binding site, presumably to stabilize the ligand inside the cavity and to protect it from the solvent. Our work has confirmed that although there are no large structural changes after mutating this conserved Trp, this amino acid residue does in fact play an important role in catalysis and in maintaining the protein stability in this class of proteins.

Role of the C-terminal tail

In our previous study, we demonstrated that the antigenicity of TCS can be reduced without a large compromise of activity by coupling a C-terminal residue, Gln219, to polyethylene glycol (He *et al*., 1999) or by the deletion of the C-terminal residues (Chan *et al*., 2000). These approaches to reduce the antigenicity of TCS were successful since the C-terminal domain is far away from the active site. The crystal structure of TCS-C7 determined in the present study has confirmed that deletion of the C-terminal residue does not affect the active site structure of TCS.

The major role of the C-terminal tail appears to be to stabilize the structure of TCS. Deletion of the last seven residues of TCS results in a large reduction, ~5 kcal/mol, in free energy of unfolding (Chan *et al*., 2000), and the accumulation of a partially structured intermediate at 2–3 M GnHCl. Since the C-terminal tail forms a number of interactions bridging the C- and the N-terminal domains (in particular, helix 7 and the hairpin of strands 2 and 3), it is reasonable to hypothesize that removal of the tail destabilizes the C-terminal domain and H7. Circular dichroism data suggest that the intermediate retains ~75% helical structure, which can be accounted for if helix 7 and the C-terminal domain are unfolded. It is likely that the partially structured intermediate retains a structured N-terminal domain that is further unfolded only when the concentration of GnHCl reaches ~4 M.

The antigenicity, measured by binding the anti-TCS mAB (IC_{50}) of TCS-C7, was 0.3 μM compared with 0.1 μM for the WT. The IC_{50} for ribosome-inactivating activities of C7 and WT-TCS were 1.8 and 0.17 nM, respectively. Although the activity of TCS-C7 is reduced ~10-fold to 1.8 nM, it should still be a very strong RIP at micromolar concentrations where antigenicity matters. Also, while TCS-C7 may not be effective as a drug at this stage, our work has shown that the C-terminal

region has a role in antigenicity and this will help us to modify it further.

Role of the hydrogen bonds related to Leu240

Our experiments to systematically delete the C-terminal residues have shown that TCS-C8 and TCS-C9 (with the last eight and nine residues deleted, respectively) were expressed solely as inclusion bodies and they cannot be refolded to the native conformation. Deleting residues 240 and 239 results in a complete loss of the hydrogen bonds between the tail of the C-terminal domain and N-terminal domain, thus the entire molecule cannot be refolded to its native conformation. This shows that the tail of the C-terminus, especially the three remaining hydrogen bonds in TCS-C7, plays an important role in maintaining the link between the N- and C-terminal domains and is required for the folding of TCS.

Compared with TCS-C7, the hydrogen bond between Leu239 and Trp192 NE1 disappears in TCS-C7-W192F, which can be refolded to native conformation successfully. On the other hand, TCS-C8 cannot be refolded to native conformation. There is only one amino acid difference between TCS-C8 and TCS-C7, Leu240, which leads to the absence of two hydrogen bonds related to Leu240. These results suggest that the hydrogen bonds formed by residue Leu240 are the key in maintaining the link between N- and C-terminal domains in TCS-C7.

The TCS-C7 coordinates have been deposited in the Protein Data Bank with accession code 1J4G.

Acknowledgements

This research was supported by the grants project '863' no. 2001AA233011 and project '973' no. G1999075602 and partially supported by a grant (CUHK 4145/01M) from the Research Grants Council of Hong Kong.

References

Bradley,J.L. and McGuire,P.M. (1990) *Int. J. Pept. Protein Res.*, **35**, 365–366.

Brunger,A.T. *et al.* (1998) *Acta Crystallogr. D Biol. Crystallogr.*, **54**, 905–921.

Byers,V.S., Levin,A.S., Waites,L.A., Starrett,B.A., Mayer,R.A., Clegg,J.A., Price,M.R., Robins,R.A., Delaney,M. and Baldwin,R.W. (1990) *AIDS*, **4**, 1189–1196.

Chan,S.H., Shaw,P.C., Mulot,S.F., Xu,L.H., Chan,W.L., Tam,S.C. and Wong,K.B. (2000) *Biochem. Biophys. Res. Commun.*, **270**, 279–285.

Endo,Y. and Tsurugi,K. (1987) *J. Biol. Chem.*, **262**, 8128–8130.

Endo,Y., Mitsui,K., Motizuki,M. and Tsurugi,K. (1987) *J. Biol. Chem.*, **262**, 5908–5912.

Gao,B., Ma,X.Q., Wang,Y.P., Chen,S.Z., Wu,S. and Dong,Y.C. (1994) *Sci. China B*, **37**, 59–73.

He,X.H., Shaw,P.C., Xu,L.H. and Tam,S.C. (1999) *Life Sci.*, **64**, 1163–1175.

Huang,Y.L. (1987) *Zhong Xi Yi Jie He Za Zhi*, **7**, 154–155.

Jimenez,A. and Vazquez,D. (1985) *Annu. Rev. Microbiol.*, **39**, 649–672.

Jones,T.A., Zou,J.Y., Cowan,S.W. and Kjeldgaard,M. (1991) *Acta Crystallogr. A*, **47**, 110–119.

Katzin,B.J., Collins,E.J. and Robertus,J.D. (1991) *Proteins*, **10**, 251–259.

Laskowski,R.A., Macarthur,M.W., Moss,D.S. and Thornton,J.M. (1993) *J. Appl. Crystallogr.*, **26**, 283–291

Li,H.G., Xu,S.Z., Wu,S., Yan,L., Li,J.H., Wong,R.N., Shi,Q.L. and Dong,Y.C. (1999) *Protein Eng.*, **12**, 999–1004.

Li,X., Ding,Y., Too,H., Wang,Z., Liu,Y., Dong,Y., Shaw,P. and Rao,Z. (2002) *Protein Pept. Lett.*, **9**, 267–273.

Lu,P.X. and Jin,Y.C. (1990) *Chin. Med. J. (Engl).*, **103**, 183–185.

McGrath,M.S. *et al.* (1989) *Proc. Natl Acad. Sci. USA*, **86**, 2844–2888.

Otwinowski,Z. and Minor,W. (1997) *Macromol. Crystallogr. Pt A*, **276**, 307–326.

Shaw,P.C., Chan,W.L., Yeung,H.W. and Ng,T.B. (1994) *Life Sci.*, **55**, 253–262.

Stirpe,F. and Barbieri,L. (1986) *FEBS Lett.*, **195**, 1–8.

Stirpe,F., Bailey,S., Miller,S.P. and Bodley,J.W. (1988) *Nucleic Acids Res.*, **16**, 1349–1357.

Wong,K.B., Ke,Y.B., Dong,Y.C., Li,X.B., Guo,Y.W., Yeung,H.W. and Shaw,P.C. (1994) *Eur. J. Biochem.*, **221**, 787–791.

Yeung,H.W., Li,W.W., Feng,Z., Barbieri,L. and Stirpe,F. (1988) *Int. J. Pept. Protein Res.*, **31**, 265–268.

Zhang,X.J. and Wang,J.H. (1986) *Nature*, **321**, 477–478.

Received November 27, 2002; revised March 7, 2003; accepted March 23, 2003